Macromolecules

Article

Cite This: *Macromolecules* XXXX, XXX, XXX−XXX

High Efficiency Luminescent Liquid Crystalline Polymers Based on Aggregation-Induced Emission and “Jacketing” Effect: Design, Synthesis, Photophysical Property, and Phase Structure

Yang Guo,[†,‡] Dong Shi,[§] Zhi-Wang Luo,[†] Jia-Ru Xu,[§] Ming-Li Li,[†] Long-Hu Yang,[†] Zhen-Qiang Yu,*[,‡] Er-Qiang Chen,[§] and He-Lou Xie*[,†]

[†]Key Laboratory of Advanced Functional Polymer Materials of Colleges and Universities of Hunan Province, College of Chemistry, Xiangtan University, Xiangtan 411105, Hunan Province, China

[‡]Shenzhen Key Laboratory of Functional Polymers, School of Chemistry and Environmental Engineering, Shenzhen University, Shenzhen 518060, China

[§]Key Laboratory of Polymer Chemistry and Physics of Ministry of Education, College of Chemistry and Molecular Engineering, Peking University, Beijing 100871, China

Supporting Information

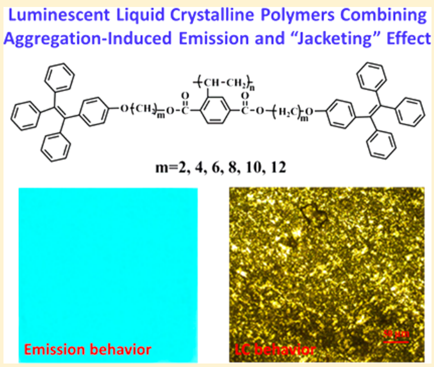

ABSTRACT: A series of high efficiency luminescent liquid crystalline polymers (LLCPs) based on aggregation-induced emission (AIE) and the “Jacketing” effect, namely, poly{2,5-bis{[2-(4-oxytetraphenylethylene)-*n*-alkyl]oxycarbonyl}styrene} (denoted as **P***m*, *m* = 2, 4, 6, 8, 10, 12), were successfully designed and synthesized via introducing tetraphenylethylene to the side group with different length spacers. Because of the AIE effect, the resultant LLCPs are completely free of aggregation caused quenching. The photophysical properties and phase behavior were studied via various techniques such as UV−vis absorption spectra, photoluminescence spectra (PL), polarized light microscopy (PLM), differential scanning calorimetry (DSC), and variable temperature one-dimensional wide-angle X-ray diffraction (1D WAXD). The results revealed that the resultant monomers showed typical AIE behavior and the polymers exhibited aggregation enhanced emission (AEE) behavior. Moreover, due to the “Jacketing” effect, the polymers showed high efficiency luminescence in the liquid crystalline state, which was significantly dependent on the spacer length (the solid-state quantum yields decreased from 52% to 18% with increasing spacer length). Meanwhile, the glass transition temperatures (T_g) decreased with increasing the length of spacers. With increasing the spacer length, the phase structure transformed from smectic A (SmA) (**P***m*s, *m* = 2, 4, 6) to hexagonal columnar phase ($\mathrm{Col_H}$) (**P***m*s, *m* = 8, 10, 12). All the polymers presented good film-forming property and processing performance, which made them be promising materials for the luminescent devices.

INTRODUCTION

Luminescent liquid crystals (LLCs) combining intrinsic light-emitting property and liquid crystalline ordering have been attracted growing interests in the past decades because of their potential applications as emissive liquid crystal displays (LCD), organic light-emitting diode (OLED), sensors, and optical information storage.[1−6] Particularly, LLCs can emit linear or circular polarized luminescence (CPL) after orientation.[4,7−12] Thus, some devices fabricated by this kind of material can show deeper color saturation, wider viewing angle, higher contrast ratio, and lower power consumption. However, the preparation of LLCs is a challenging problem because the regularly packed chromophoric mesogens lead to the aggregation caused quenching (ACQ) effect.[13−21]

Different from ACQ, aggregation-induced emission (AIE) phenomenon[22−25] is that the aggregation leads to enhancing the emission of weak fluorophor or even nonluminescent molecules when these molecules are aggregated into particles in poor solvents or fabricated into solid state from good solvents.[26−34] At present, many AIE luminogens have been successfully developed through rational molecular design.[35−41] For example, when AIE luminogens are introduced into LCs, it may effectively resolve the conflicts between fluorophor quenching and the necessary ordered molecular packing for liquid crystallinity. Nowadays, most of the methods to fabricate the LLCs with stable LC ordered structure and high solid-state emission efficiency adopt the simple approach using the AIE-active dye as core and conventional mesogens as periphery, and the resultant LLCs can result in different supramolecular phase structures, such as columnar, nematic, smectic A (SmA), or smectic C (SmC) phase.[42−47]

Tetraphenylethylene (TPE) is a typical AIE luminogen with high solid-state efficiency and highly twisted structure, which has been extensively employed as luminogen to construct LLCs

Received: July 27, 2017
Revised: December 2, 2017

DOI: 10.1021/acs.macromol.7b01605

due to its facile synthesis and versatile functionalization.[48−51] Incorporating LC mesogens into TPE molecule may be the most efficient method to construct LLCs, and the phase structure of the resultant LLCs is strongly dependent on the structure of the LC mesogens. For example, Tang and co-workers[49] designed and synthesized a series of LLC polymers (LLCPs) containing biphenyl and TPE units by click polymerization because the biphenyl groups could be easily packed to form LC phase and TPE group could be forced to be packed in the confined space; thus, the resultant LLCPs showed both high solid-state efficiency and LC property.[48,49,52−57]

Different from the generally method of synthesizing LLCPs by copolymerizing mesogens and luminogens, herein, we propose a new approach to fabricate LLCPs based on AIE and the side-chain "Jacketing" effect. According to the previous works,[58,59] mesogen-jacketed liquid crystalline polymers (MJLCPs) are a kind of LCPs with bulky side group directly attached to the polymer main chain or via very short spacer, whether the bulky side group is mesogenic or not. Because of the spatial requirement of the bulky side groups, the whole polymer chain is enforced to take extended conformation along the main-chain direction.[60] Thus, the resultant polymer chain forms a cylinder-like or ribbon-like single conformational unit because the side groups and the backbone of MJLCPs almost merge together.[61−63] We anticipate that when the periphery of MJLCP is modified by TPE, the rigid MJLCP will restrict the intramolecular rotation of TPE and the resultant LLCPs will form luminescent columnar or smectic structure.

With this in mind, we designed and successfully synthesized poly{2,5-bis{[2-(4-oxytetraphenylethylene)*n*-alkyl]-oxycarbonyl}styrene} (denoted as **P***m*, *m* = 2, 4, 6, 8, 10, 12). The chemical structure is shown in Scheme 1. **P***m* can be easily achieved via radical polymerization due to the monomers containing polymerizable vinyl. The chemical structures of the monomers and polymers have been confirmed by FTIR, ^{1}H NMR, ^{13}C NMR, mass spectral, and elemental analysis, and the molecular weight of the polymers determined by gel permeation chromatography (GPC). UV−vis and photoluminescence spectra (PL) results indicated that the monomers were AIE active and polymers exhibited AIE or aggregation enhanced emission (AEE) characteristics. Further, on the basis of polarized light microscope (PLM), differential scanning calorimetry (DSC), and wide-angle X-ray diffraction (WAXD) results, we found that the LLCPs formed SmA (**P***m*s, *m* = 2, 4, 6) or hexagonal columnar phase (Col$_H$) (**P***m*s, *m* = 8, 10, 12).

Scheme 1. Molecular Structures of the LLCPs (P*m*s)

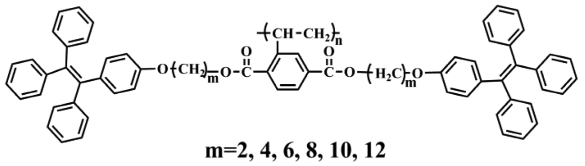

m=2, 4, 6, 8, 10, 12

■ EXPERIMENTAL SECTION

Materials. 1,12-Dibromododecane, 1,10-dibromodecane, 1,8-dibromooctane, 1,6-dibromohexane, 1,4-dibromobutane, 1,2-dibromoethane, benzophenone, 4-hydroxybenzophenone, zinc powder, and titanium tetrachloride were purchased from Energy Chemical and directly used. Tetrahydrofuran (THF) was refluxed over sodium and distilled before use. Acetone, *N*,*N*-dimethylformamide (DMF), potassium carbonate, and potassium bicarbonate were purchased from Guangdong Guanghua Sci-Tech Co., Ltd., and were used directly. 2,2-Azobis(isobutyronitrile) (AIBN) was purified by recrystallization using ethanol as solvent. 2-Vinyl-*p*-biphthalic acid was synthesized in our lab.[64]

Instruments and Measurements. ^{1}H NMR and ^{13}C NMR experiments were carried out on a Bruker ARX400 spectrometer, where deuterated chloroform (CDCl$_3$) was used as the solvent and tetramethylsilane (TMS) as the internal standard. Fourier transform infrared spectroscopy (FTIR) spectra were recorded in KBr pellets on a PE Spectrum One FTIR spectrometer. Mass spectral and elemental analysis experiments were performed on Autoflex III and Varlo EL III, respectively. A GPC (Waters GPC1515) experiment was carried out to determine the apparent number-average molecular weight (M_n) and molecular weight distribution (M_w/M_n), where THF was used as the eluent and the linear polystyrene as standard was used to calibrate the standard curve.

UV−vis absorption spectra were recorded on a Cary 100 using the Flashing xenon lamp as the light source. Emission spectra were measured on a spectrofluorometer QM40 in the right-angle geometry with 1 cm quartz cuvettes. The wavelength of the excitation light fixed was λ_{ex} = 365 nm, and the slit width of 5 nm was used for both monochromators. The quantum yields ($\Phi_{F's}$) in the solid state were determined using an integrating sphere on a Nanolog FL3-2iHR infrared fluorescence spectroscopy equipped with R928 photomultiplier as detector.

Thermogravimetric analysis (TGA) was carried out on a TA SDT 2960 instrument under a nitrogen atmosphere at a heating rate of 20 °C/min. DSC experiment was performed on a TA DSC Q100

Scheme 2. Synthetic Route of the Monomers and Polymers

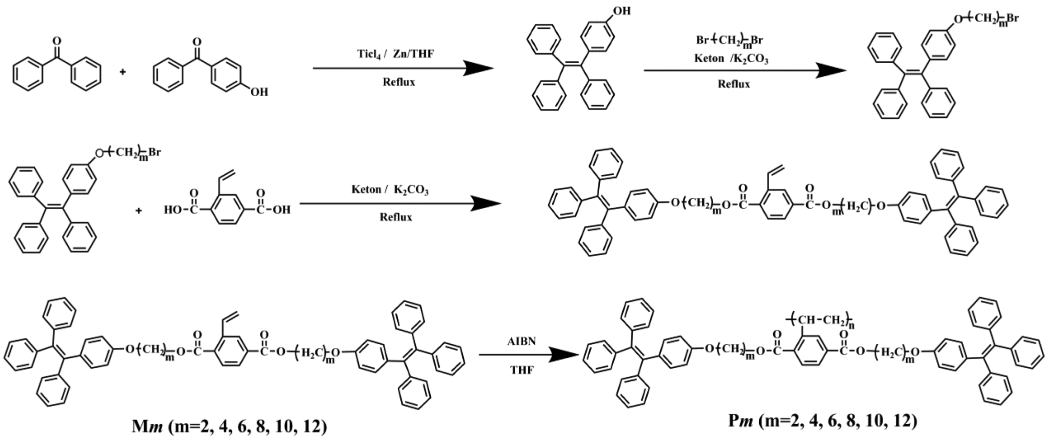

DOI: 10.1021/acs.macromol.7b01605
Macromolecules XXXX, XXX, XXX−XXX

calorimeter with a programmed heating procedure in nitrogen. The LC texture of the samples was investigated under PLM (Leica DM-LM-P), which was equipped with a Mettler FP82HT hot stage. 1D-WAXD powder curves were recorded on a Bruker D8 advance diffraction equipped with a temperature control unit (Paar Physica TCU 100). In WAXD experiment, the sample was set horizontally on the stage and the silver behenate ($2\theta < 10°$) was used to calibrate the reflection peak position.

Synthesis. The synthetic route of **P***m*s and monomers (**M***m*s) is shown in Scheme 2. The syntheses of different monomers and polymers were similar; herein we use 2,5-bis{[2-(4-oxy-tetraphenylethylene)-6-hexane]oxycarbonyl}styrene (**M6**) and the corresponding **P6** as the example to elucidate this synthetic process. The detailed synthesis information was described as follows. For other monomers and polymers, the relevant synthetic data are presented in the Supporting Information.

Synthesis of 4-Hydroxytetraphenylethylene. The mixture of benzophenone (2 g, 10 mmol), 4-hydroxybenzophenone (2.2 g, 12 mmol), zinc powder (2.9 g, 44 mmol), and THF (200 mL) was added into a 500 mL round-bottom flask. After stirring for 0.5 h, $TiCl_4$ (2.5 mL, 22 mmol) was added to round-bottom flask dropwise under a N_2 atmosphere in salt−ice bath conditions. One hour stirring later, the reaction was refluxed for 12 h. When the reaction mixture was cooled to 25 °C, 10% aqueous K_2CO_3 solution (100 mL) was dropped into the mixture and then vigorously stirred for 5.0 min. Afterward, the dispersed insoluble material was removed by filtrating. The mixed solution was extracted with CH_2Cl_2 (3 × 50 mL), and the organic layer was collected. The combined organic fractions were washed with water and dried with Na_2SO_4. The solvent of the combined organic fractions was removed by rotary evaporators. The crude product was further purified by column chromatography with silica gel as adsorbed phase and with petroleum ether/CH_2Cl_2 (5:1, v/v) as eluent. The resultant product (TPE-OH) is white solid with the yield of 44.2%. ^1H NMR (DMSO-d_6) δ (ppm): 9.35 (s, 1H, −OH), 7.1 (d, 9H), 6.98 (s, 6H), 6.73 (s, 2H), 6.51 (s, 2H).

Synthesis of *ω*-(4-Tetraphenylethylene-yloxy)-1-bromohexane. The mixture of 4-hydroxytetraphenylethylene (3 g, 8.6 mmol), 1,6-dibromohexane (5 mL, 0. 013 mol), potassium carbonate (1.79 g, 0.013 mol), and 100 mL of acetone was added into a 250 mL round-bottom flask with continuous magnetic stirring at 60 °C overnight. After the reaction was complete, the product was dropped into cold water to precipitate and then filtered. The crude product was purified by recrystallization with petroleum ether to yield the white powder. Yield: 80%. ^1H NMR ($CDCl_3$) δ (ppm): 7.13−7.07 (m, 9H), 7.05−6.99 (m, 6H), 6.91−6.87 (m, 2H), 6.59−6.54 (m, 2H), 3.88 (m, 2H,−OCH_2−), 3.42 (m, 2H, −OCH_2−Br), 1.95−1.85 (m, 2H, −CH_2−), 1.80−1.71 (m, 2H, −CH_2−), 1.50 (m, 4H, −CH_2−).

Synthesis of 2,5-Bis{[2-(4-oxytetraphenylethylene)hexane]-oxycarbonyl}styrene (M6). 2-Vinyl-*p*-biphthalic acid (0.7 g, 40 mmol), $KHCO_3$ (5.0 g, 50 mol), *ω*-(4-tetraphenylethyleneyloxy)-1-bromohexane (4.1 g, 80 mmol), and 100 mL of *N*,*N*-dimethylformamide (DMF) were added into a 250 mL bottom flask, and the mixture was reacted at 100 °C for 24 h. Afterward, the reaction mixture was cooled to room temperature and pump filtered. The filter liquor was poured slowly into cold water, and then solid precipitation was further pump filtered. The crude product was purified by column chromatography, and a white solid product was obtained. Yield: 70%. ^1H NMR ($CDCl_3$) δ (ppm): 8.26 (s, 1H, Ar−H), 7.99 (d, 2H, Ar−H), 7.13−7.00 (m, 31H), 6.93 (m, 4H), 6.63 (m, 4H), 7.38 (s, 1 H, −CH=CH_2), 5.75 (d, 1 H, −CH=CH_2), 5.42 (d,1 H, −CH=CH_2), 3.88 (m, 4H, −OCH_2−), 3.42 (m, 4H, −OCH_2−), 1.95−1.85 (m, 4H, −CH_2−), 1.80−1.71 (m, 4H, −CH_2−), 1.50 (m, 4H, −CH_2−), 1.77 (m, 4 H, −CH_2−). ^{13}C NMR: 166.8 ($\underline{C}$=O), 165.7 ($\underline{C}$=O), 157.41 (TPE $\underline{C}$−O), 144.04 (TPE −$\underline{C}$=C−), 139.57−140.5 (TPE C−$\underline{C}$=C−C), 136.18 (phenyl $\underline{C}$−C=C), 134.91 (aromatic $\underline{C}$−C=O), 132.58 ($\underline{C}$−C=C), 131.36, 130.31, 128.09, 127.71, 127.61, 126.37, 126.25 (TPE $\underline{C}$), 117.79 (aromatic $\underline{C}$), 113.54 (TPEC, $\underline{C}$−C=C), 67.00 (TPE−O$\underline{C}H_2$−), 65.14 (−O$\underline{C}H_2$−), 65.14 (−O$\underline{C}H_2$− aromatic), 25.55−25.98 (−$\underline{C}H_2$−). IR (ATR, cm^{-1}): 3051, 985.57 (HC=CH_2) 2930.51, 2857.41 (−CH_2−), 3051.32, 1603.64, 1491.57, 759.93, 746.77, 696.18 (−Ar), 1716.25 (C=O), 1174.06 (C−O−C), 1387.71, 842.45 (−C=C−). Anal. Calcd for $C_{74}H_{68}O_6$: C, 84.41, H, 6.46, O, 9.13. Found: C, 84.45, H, 6.80, O, 8.75. MS: MALDI-TOF MS (CCA matrix in THF, laser λ = 337 nm, + mode) for $C_{74}H_{68}O_6$ calcd 1052.5 Da, found m/z 1052.5 $[M]^{\bullet +}$.

Synthesis of Poly{2,5-bis{[2-(4-oxytetraphenylethylene)-hexane]oxycarbonyl}styrene}(P6). 1.052 g (1 mmol) of **M6**, 1 mg/mL chlorobenzene solution of AIBN (0.1 mL), and chlorobenzene (1.0 mL) were transferred into a reaction tube; the tube was purged with nitrogen, subjected to three freeze−thaw cycles to remove oxygen, and then sealed off under vacuum. The polymerization reaction was carried out at 90 °C for 24 h. Afterward, after opening the tube, the reaction product was diluted with 30 mL of THF. The resultant substance was precipitated in methyl alcohol. To completely remove the unreacted monomers, the precipitated procedure was repeated several times until the monomer peak could not be detected by ^1H NMR. The product was dried under vacuum. Yield: 85%.

■ RESULTS AND DISCUSSION

Synthesis and Characterization of the Monomers and Polymers. The monomers were successfully synthesized through multistep reactions according to Scheme 2, and their chemical structures were confirmed by various characterization techniques. All monomers with vinyl could be polymerized readily using the radical polymerization method. The resultant polymers presented the sufficient large molecular weight (MW) to eliminate the effect of MW on the phase behavior and luminescent property. Both the monomers and polymers are well soluble in common organic solvents such as toluene, THF, chloroform, and chlorobenzene. As shown in Figure 1 of ^1H NMR, the resonance signals of **M6** at 8.26 ppm (peak e) and 7.93 ppm (peak d) are the characteristic peaks of hydrogen displacement of the benzene ring linked with a vinyl group, those at 5.4 ppm (peak a), 5.8 ppm (peak b), and 6.6 ppm (peak c) are characteristic peaks of vinyl substituent, and those at the 6.93−7.28 ppm (peak l, m, n, o, p, q, r, s, t) are the characteristic peaks of hydrogen displacement of TPE. The area ratios of all peaks are well consistent with the number of hydrogen atoms. For **P6**, the distinct variation is the disappearance of the peak (a, b, c) of the vinyl substituent. In the meantime, some peaks of **P6** become quite broad compared to the corresponding peaks of **M6**, consistent with the expected polymer structure. The detail results of other monomers and polymers are shown in the Supporting Information. GPC was further used to determine the MWs

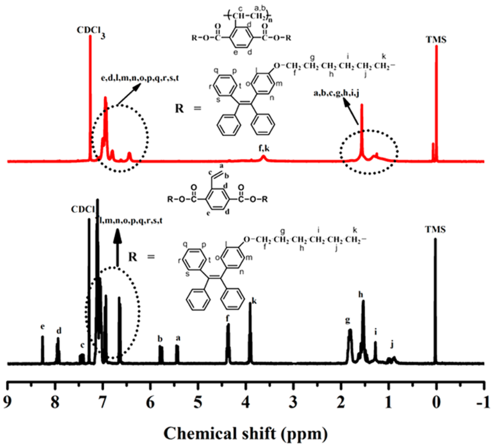

Figure 1. ^1H NMR spectra of **M6** and **P6**.

and the polydispersity index of **P***m* (GPC curves is shown in Figure S1), and the relevant data are outlined in Table 1.

Table 1. GPC, DSC, and TGA Result of P*m* (*m* = 2, 4, 6, 8, 10, 12)

sample	yield[a] (%)	$M_{n,GPC}$[b] (×10^5)	M_w/M_n[b]	T_g (°C)[c]	$T_{d,N2}$[d] (°C)
P2	95	4.03	1.72	122	377
P4	85	4.12	1.56	95	365
P6	85	3.96	1.72	79	355
P8	87	4.82	2.01	69	364
P10	88	5.21	2.13	57	359
P12	86	4.76	1.78	51	352

[a] According to weight calculation. [b] From GPC instrument. [c] From DSC at a rate of 10 °C/min under heating. [d] The temperature at 5.00% weight loss.

Phase Transitions and Supramolecular Ordered Structures. The thermal stability of **P***m*s (*m* = 2, 4, 6, 10, 12) was investigated by TGA. The results indicated that the temperatures at 5% weight loss for all polymers were higher than 350 °C in nitrogen atmosphere, implying that these LLCPs showed very good thermal stabilities. Subsequently, DSC experiments were performed to investigate phase transitions of the monomers and polymers. To erase the thermal history, all the samples were first heated to 260 °C at a rate of 20 °C/min followed by isothermal annealing for 10 min. Then, the first cooling trace and the second heating trace were recorded at 10 °C/min. For all monomers and polymers only a single glass transition temperature (T_g) could be observed during the heating or cooling process (see Figure 2 and Figure S2), similar to that found in other MJLCPs.[60] Meanwhile, the glass transition temperature (T_g) for the polymers gradually decreased with increasing the alkyl spacer length, which meant that increased alkyl spacer length could lead to better molecular mobility. The detailed information is shown in Table 1. The result well agreed with the previous works about the ionic polymeric liquid crystals (IPLCs).[64,65]

PLM results revealed that at room temperature all samples could not show birefringence phenomenon. For **P2**, **P4**, and **P6**, with temperature increased to higher than T_g, the distinct birefringence could be observed and did not disappear before decomposition during heating (see Figure 3a−c), and during cooling the birefringence always maintained. For **P8**, **P10**, and **P12** with longer flexible spacer, no birefringence was observed during the whole heating process, but applying shear force, the birefringence phenomena immediately appeared (see Figure 3d−f). We speculated that the LC domains in these polymers were too small to be observed, and the external stimuli could induce the small LC domains agglomerate to enough bigger domain. Once the bigger domain formed, it could be always maintained during cooling. This phenomenon might imply the polymers formed two different supramolecular ordered structures.

While DSC and PLM experiments did not provide more information on the phase behavior of **M***m*s and **P***m*s, we carried out the temperature-variable 1D-WAXD experiments to elucidate phase structures and insight into their molecular packing. The results revealed all monomers were amorphous, and all polymers showed supramolecular ordered structures. Figure 4a,b illustrates two sets of 1D-WAXD diffractogram of the as-cast film of **P2**. During the first heating process, at 30 °C two peaks in the low-angle region at 2θ = 3.44° and 6.79° and one diffused halo in the high-angle region at approximately 2θ = 20° were observed. The ratio of the diffraction vectors of the low-angle peaks was 1:2, which indicated smectic phase with a period of 2.56 nm. The high-angle amorphous halo indicated the subnanometer structure was disordered. Presuming the alkyl spacer was *all-trans*, the calculated molecular width was 3.3 nm, and the width of TPE molecular was 0.69 nm; thus, we could speculate **P2** formed the SmA phase with TPE interdigitated each other. During the whole heating cooling process, both the low-angle peaks and the high-angle halo always remained unchanged. The ratio of the vectors of the diffraction peaks q_1:q_2 also remained as 1:2, indicating the stable smectic phase in whole temperature range. Figure 4c,d shows the 1D-WAXD diffractogram of **P6**. Two peaks were showed in the low-angle region at 2θ = 3.13° and 6.31° in addition to a one diffuse halo in the high-angle region. Likewise, the diffraction position hardly changed during both heating and cooling process. A similar result of **P4** is shown in Figure S3a,b.

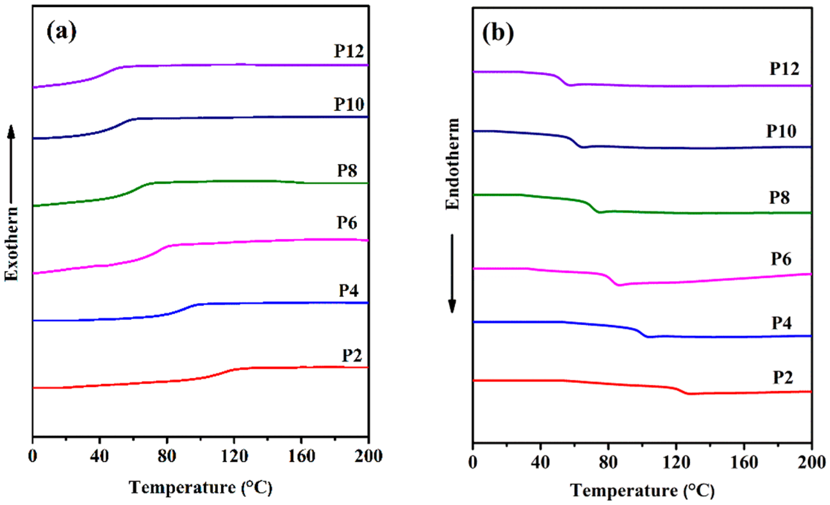

Figure 2. DSC thermograms of **P***m*s (*m* = 2, 4, 6, 10, 12) at a rate 10 °C/min during the processes of the first cooling (a) and the second heating (b).

DOI: 10.1021/acs.macromol.7b01605

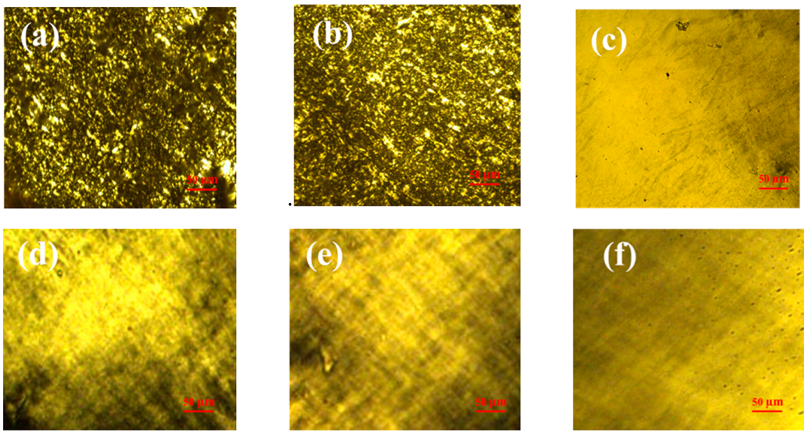

Figure 3. Representative textures of **P2** (a), **P4** (b), **P6** (c), **P8** (d), **P10** (e), and **P12** (f) at 140 °C (200× magnification).

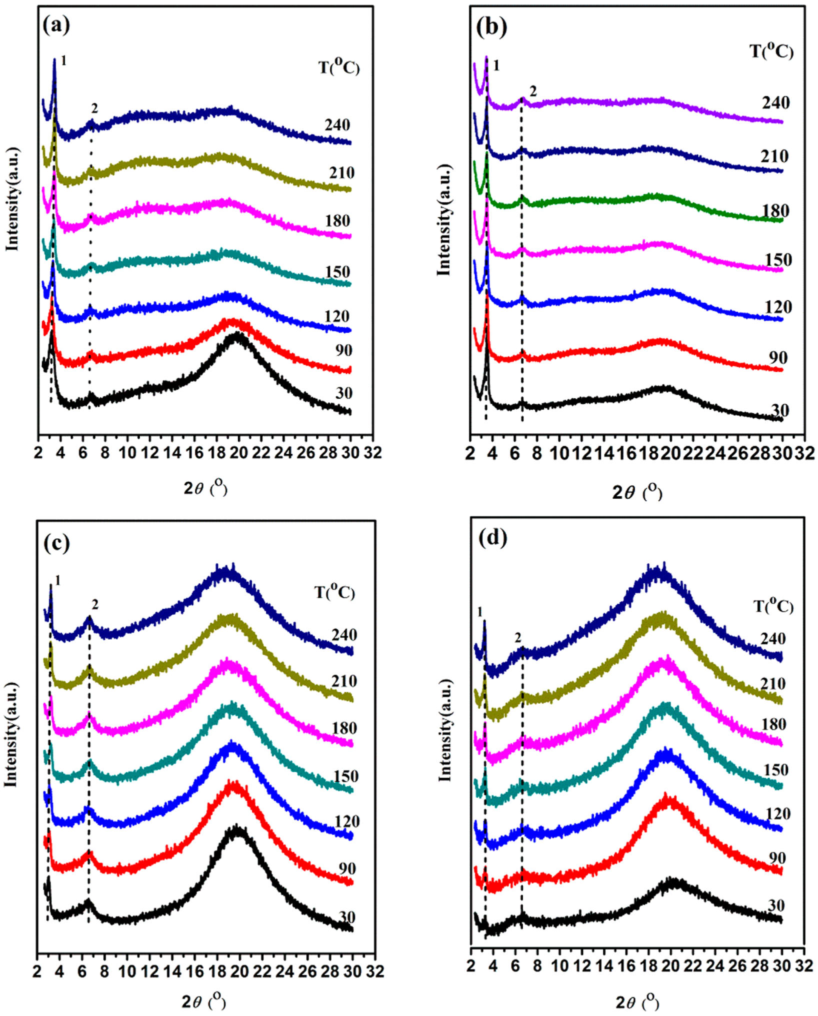

Figure 4. 1D WAXD profiles of **P2** recorded at various temperatures upon heating (a) and cooling (b) and **P6** recorded at various temperatures upon heating (c) and cooling (d).

The results indicated **P4** and **P6** also showed a similar smectic phase.

With the increase of the spacer length, **P8**, **P10**, and **P12** showed similar phase structure, which are different from that of **P2**, **P4**, and **P6**. The temperature-variable 1D-WAXD diffractograms of the as-cast film of **P8** are shown in Figure 5. During the first heating process, at 30 °C there were three low-angle diffraction peaks at 2θ = 3.11°, 5.44°, and 6.33° and an amorphous halo at 2θ = 20°. The ratio of the scattering vectors of the three diffraction peaks in the low-angle region was $1:3^{1/2}:2$, suggesting the LC structure of hexagonal columnar ($\mathrm{Col_H}$) phase. With increasing the temperature, the intensity of the first-order peak increased slightly, and the second- and third-order peaks became more obvious. Similar to the samples

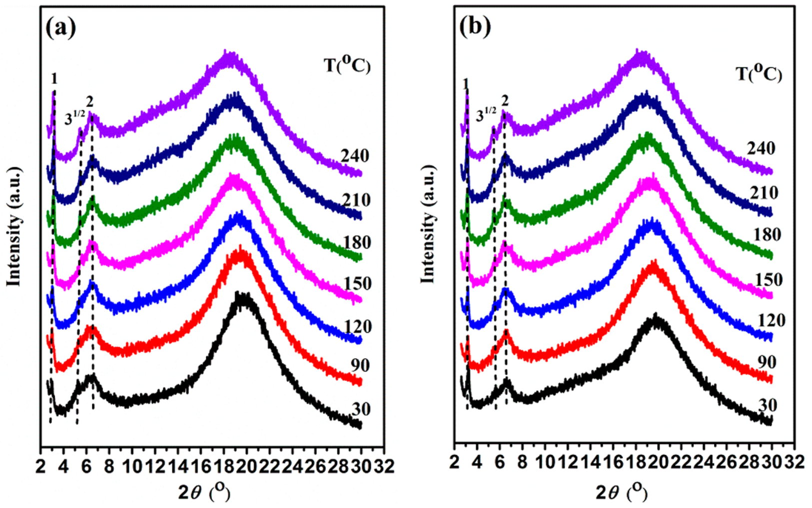

Figure 5. 1D WAXD profiles of **P**8 recorded at various temperatures upon heating (a) and cooling (b).

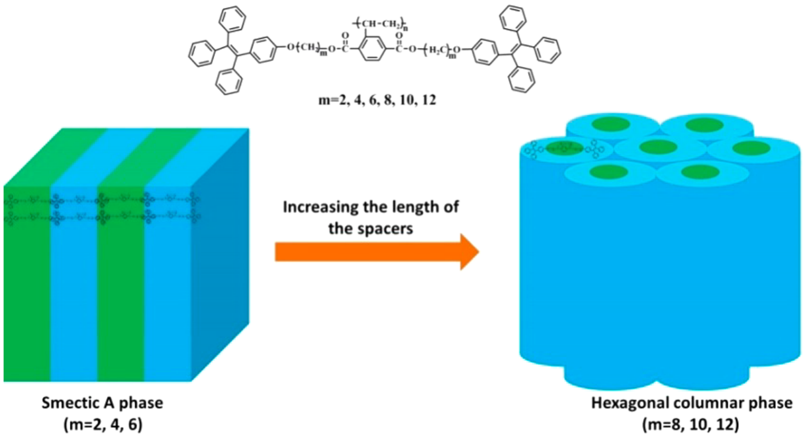

Figure 6. Schematic of the smectic structure and the Col_H structure of **P***m*s.

P4 and **P**6 discussed above, the diffraction peaks and halo remained unchanged during the whole temperature-variable process. That meant **P**8 formed the stable Col_H phase during the whole temperature-variable region. For **P**10 and **P**12, they also formed Col_H phase at different temperatures, and they showed a similar transition during the heating process. The detailed information is shown in Figure S3c−f.

The WAXD results revealed that **P***m*s could form two different types of LC phases, i.e., SmA and Col_H phase, depending on the length of the alkyl spacers (see Figure 6). The phase behavior of **P***m*s was similar to that we previously reported for ILCPs with different the flexible spacer length.[65] Thus, for **P**2, **P**4, and **P**6, the short flexible spacer between side-group TPE and polystyrene backbone resulted in the main chain and side chain as an integral to form a ribbon-like molecule. In this case, the TPE groups interdigitatedly packed, which favored forming smectic phase. For **P**8, **P**10, and **P**12, because of the long alkyl spacers, the side-group TPE decoupled from the main chain, the main chain of the polystyrene derivative formed column structure, and the side-group TPE surrounded the main chain. Thus, the molecules of **P**8, **P**10, and **P**12 preferred to form cylinders as a whole, and then the cylinders packed to form the Col_H phase. Moreover, it is worth noting that as-cast MJLCPs are often amorphous, and their LC structural development requires the treatment of high temperature. In this system, however, we found the as-cast film could form LC ordered structure, meaning the solvent could induce the ordered structure formation. We presume that it is due to that the strong aggregation of TPE molecules facilitates the formation of the ordered structures in the as-cast film.

Photophysical Properties. The photophysical properties of the monomers and the corresponding polymers were investigated in THF solution and thin film. The absorption spectra of THF solutions of **M***m*s and **P***m*s at a concentration of 10^{-5} mol/mL are shown in the Supporting Information. The maximum absorption for the solutions of monomers occurred at 246 and 316 nm, which was attributed to the typical absorption of TPE group (see Figure S4a). After polymerization, the polymers solutions exhibited nearly the same absorption behavior as that of the monomers (see Figure S4b). This was mainly due to the structural similarity. Note that the TPE luminogens were separated from the polystyrene backbone by the alkyl spacers, which hindered their electronic interactions.

Because of the incorporation of the AIE luminogens, the monomers and polymers were expected to be AIE or AEE active. First, the emission behaviors of monomers were investigated in solvent/nonsolvent mixtures. Herein, the **M**6 was used as example to illustrate this process. No luminescence could be observed in THF solution (see Figure 7). However,

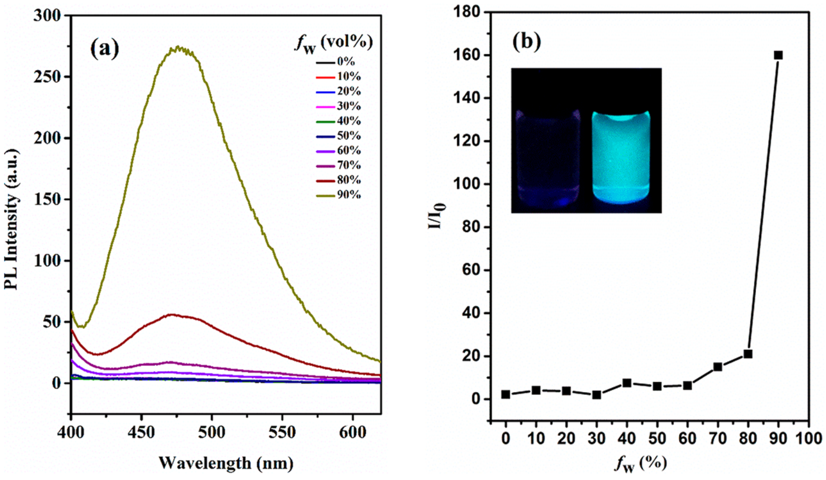

Figure 7. (a) Emission spectra of **M6** in THF/H_2O with varied water content. (b) Plots of I/I_0 values depended on water content at 476 nm for **M6**; the inset photos of **M6** taken under UV light in THF with 0 and 90% water contents.

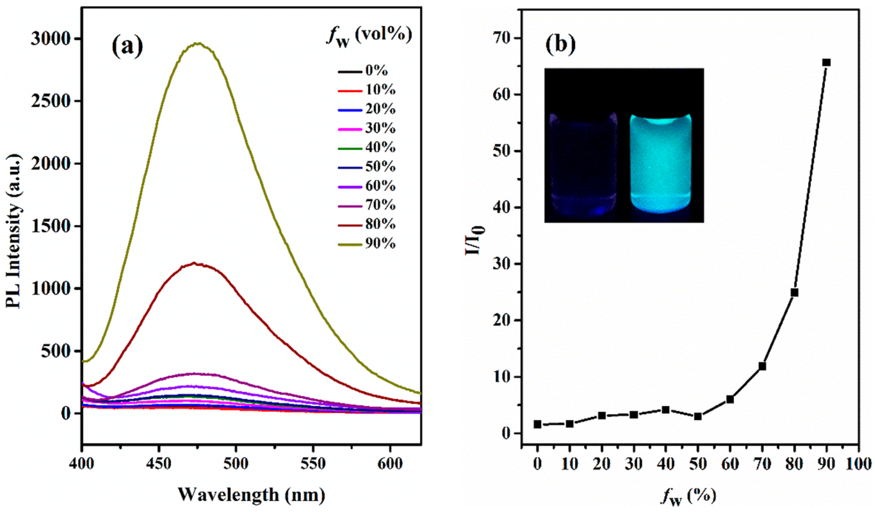

Figure 8. (a) Emission spectra of **P6** in THF/H_2O mixtures with varied water fractions. (b) Plots of I/I_0 values versus water contents of the aqueous mixtures at 476 nm for **P6**; the inset photos of in THF with 0 and 90% water fractions taken under UV light.

with gradually adding water into the THF solution, when water content achieved 40%, the mixture begins to turn on the emission. Further increasing the water content could distinctly enhance its luminescence evidenced by the PL spectra. When the water content achieved 80%, the emission intensity with the maximum at 476 nm was approximately 20-fold than that in the THF solution. Furthermore, when the water content achieved 90%, the emission intensity with the maximum at 476 nm underwent a drastic increase, which arrived almost 160-fold than that in the THF solution. Because of the benzene ring connecting to the vinyl emitted in the UV region, the visible emission of **M6** should be attributed to the TPE units. Likewise, other monomers were also nonluminescence in THF solution, and the addition of water resulted in AIE behaviors (detailed information is shown in Figure S6).

Sequentially, the AIE behaviors of the polymers were also investigated. As shown in Figure 8, **P6** was extremely weak luminescent in THF solution but exhibited the sky-bluish emission with the maximum at 476 nm in the THF/water mixture solution. The emission intensity gradually enhanced with increasing the water content in the mixture solution. For 70% and 80% water content, the emission intensity with the maximum at 476 nm of **P6** in the mixture solvent were approximately 15- and 20-fold than that in the THF solution, respectively. When the water content achieved 90% in the aqueous mixtures, the emission intensity was 66-fold higher than that in THF solution. The analogous experimental phenomenon has been observed in other polymers (see Figure S6). However, compared with the emission behavior of all polymers in THF solution, it could be found that **P8**, **P10**, and **P12** were hardly luminescent, but **P2**, **P4**, and **P6** could emit weakly.

We found that the emission efficiency for both the monomers and polymers had the dependence of molecular structures. Figures S7a and S7b show the emission spectra at 90% water content of the monomers and polymers, respectively. Overall, the monomers had the emission intensity decreased with the increase of the spacer length between the TPE and the styrene headgroup. For the polymers, the emission intensity also gradually decreased with the increase of the spacer length. However, for the solution with the same molar concentration of TPE group, the comparison of the values of PL intensity suggested that the emission of the polymers was much stronger than that of the monomers. The value of the emission intensity of the polymers was approximately ~10 times larger than that of the corresponding monomers. Meanwhile, the data shown in Figure S7 also indicated the increments with the decrease of spacer length for polymers were much higher than that of the monomers.

For insight into the relationship between luminescent behavior and chemical structures, each emission curve of the above-mentioned emission spectra at 90% water content were integrated, which was directly dependent on the emission efficiency. The values of the integral areas showed a similar tendency as that discussed above, which is shown in Figure 9.

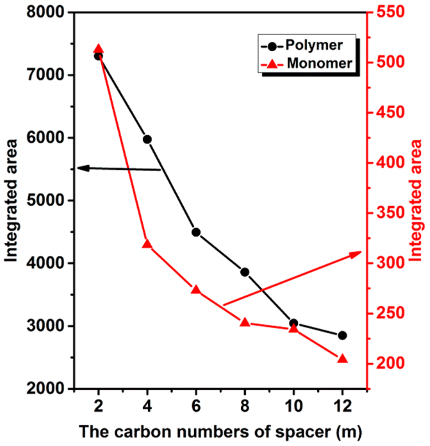

Figure 9. Integral area of emission spectra at 90% water content of the aqueous mixtures for monomers and polymers.

The integral areas of both the monomers and polymers decreased with the length of spacer increased, and the values of polymers were also much larger than those of the monomers. Clearly, the emission efficiency of the polymers was significantly enhanced compared to that of their corresponding monomers. The enhancement of the emission efficiency for the polymers mainly attributed to the spatial hindrance of the intramolecular rotation of the side-chain TPE groups. On the other hand, for both monomers and polymers, the emission intensity gradually receded with increasing the length of spacer, but the attenuation degree for monomers was significantly less than that of the corresponding polymers. For monomers, the main reason for the attenuation was that the incorporation of electronically saturated alkyl chains was harmful to the TPE aggregation formation and the long alkyl chains more easily reduced the light emissions. For the polymers, in addition to the reason above-mentioned, the more important reason would be the spatial limitation of volume effect in these polymers. Increasing the length of spacers improved the mobility of the TPE luminogens, which resulted in the reduction of AIE effect. Thus, compared with the monomers, the polymers showed more obvious attenuation of AIE effect with the change of the spacer length.

In addition to the typical AIE behavior of the solution, all solid samples of **M***m*s and **P***m*s obtained from solution casting showed clearly luminescent behavior. For the monomers, the quantum yields ($\Phi_{F's}$) measured were 5.0%, 3.0%, 2.8%, 2.6%, 2.5%, and 2.1% determined by the integrating sphere. Compared with the typical TPE molecule, the $\Phi_{F's}$ of the monomers were very low, which might be attributed to the amorphous state. As shown in Figure 9, the values of $\Phi_{F's}$ measured were 51.9%, 41.3%, 31.7%, 27.1%, 20.0%, and 18.1% for **P2**−**P12**, which were 1 order of magnitude higher than that of monomers. As described above, all polymers showed supramolecular ordered structure, which meant they could strongly emit in the LC state.

Figure 10 shows that the $\Phi_{F's}$ values of solid **P***m*s decreased with increasing the spacer length, which was in good agreement with the variation tendency in the solution mentioned above. The WAXD experiments revealed **P2**−**P6** and **P8**−**P12** showed SmA phase and Col_H phase, respectively. Evidently, the $\Phi_{F's}$ of the polymers in SmA phase was higher than that of polymers in the Col_H phase. We estimated that the relatively higher $\Phi_{F's}$ for $m \leq 6$ was because that TPE groups could form interdigitated packing in the SmA phase, of which TPE groups were squeezed by the quite rigid environment. In the columnar phase of **P***m*s with $m \geq 8$, the TPE groups were located at the periphery of the column. This spatial arrangement provided the TEP groups more interfacial area in comparison to that in SmA phase. Consequently, the phenyl rings could be rotated more freely, which would result in the decrease of $\Phi_{F's}$.[66] Figure 9 also shows that increasing spacer length could lead to more pronounced reduction of $\Phi_{F's}$ for the samples in SmA phase compared to that in Col_H phase. This observation was in accordance with the space length dependence of T_g (see Table 1). This meant that the increase of spacer length could effectively make the sample to be soft and thus lose the restriction of TPE motion.

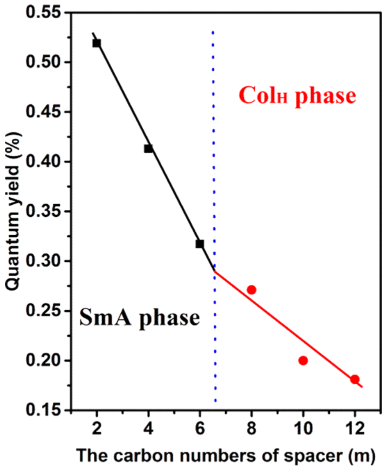

Figure 10. Relationship of **P***m*s between the quantum yields ($\Phi_{F's}$) and the spacer length.

■ CONCLUSIONS

In summary, we successfully synthesized a series of novel high efficiency luminescent liquid crystalline polymers (**P***m*s) based on AIE luminogens and the "Jacketing" effect via radical polymerization. Although all monomers and polymers showed typical AIE behavior and solid-state emission, their luminescent behavior and phase behavior were quite dependent on their structures. Because of the existence of the "Jacketing" effect, all polymers not only showed obvious luminescent behavior in LC state, but also their luminescence efficiency significantly decreased with increasing spacer length (their solid-state quantum yields from 52% to 18%). Meanwhile, the alkyl spacer length also impacted their phase behavior and phase structure. With the increase of the alkyl spacer length, the glass transition temperature (T_g) gradually decreased, and their phase structure changed from smectic A phase (**P***m*s, *m* = 2, 4, 6) to Col_H phase (**P***m*s, *m* = 8, 10, 12). The results imply that adjusting the alkyl spacers can be an effective way to control the supramolecular structures and the photophysical properties of the high efficiency luminescent liquid crystalline polymers with the "Jacketing" effect, which provides a new method to fabricate promising luminescent material.

ASSOCIATED CONTENT

Supporting Information

The Supporting Information is available free of charge on the ACS Publications website at DOI: 10.1021/acs.macromol.7b01605.

Experimental details; Figures S1−S7 (PDF)

AUTHOR INFORMATION

Corresponding Authors

*E-mail: xhl20040731@163.com (H.L.X.).
*E-mail: zqyu@szu.edu.cn (Z.Q.Y.).

ORCID

Zhen-Qiang Yu: 0000-0002-0862-9415
Er-Qiang Chen: 0000-0002-0408-5326
He-Lou Xie: 0000-0003-4103-2634

Notes

The authors declare no competing financial interest.

ACKNOWLEDGMENTS

This work is financially supported by the National Natural Science Foundation of China (21374092, 21674088, and 21674065), the Nature Science Foundation of Hunan Province (2016JJ2127), State Key Laboratory for Modification of Chemical Fibers and Polymer Materials (LK1608), and Hunan 2011 Collaborative Innovation Center of Chemical Engineering & Technology with Environmental Benignity and Effective Resource Utilization.

REFERENCES

(1) Grell, M.; Bradley, D. D. Polarized luminescence from oriented molecular materials. *Adv. Mater.* **1999**, *11*, 895−905.

(2) Hayasaka, H.; Miyashita, T.; Tamura, K.; Akagi, K. Helically π-Stacked Conjugated Polymers Bearing Photoresponsive and Chiral Moieties in Side Chains: Reversible Photoisomerization-Enforced Switching Between Emission and Quenching of Circularly Polarized Fluorescence. *Adv. Funct. Mater.* **2010**, *20*, 1243−1250.

(3) Jeong, Y. S.; Akagi, K. Liquid crystalline PEDOT derivatives exhibiting reversible anisotropic electrochromism and linearly and circularly polarized dichroism. *J. Mater. Chem.* **2011**, *21*, 10472−10481.

(4) San Jose, B. A.; Matsushita, S.; Moroishi, Y.; Akagi, K. Disubstituted liquid crystalline polyacetylene derivatives that exhibit linearly polarized blue and green emissions. *Macromolecules* **2011**, *44*, 6288−6302.

(5) Schadt, M. Linear and non-linear liquid crystal materials, electro-optical effects and surface interactions. Their application in present and future devices. *Liq. Cryst.* **1993**, *14*, 73−104.

(6) Sun, Q.; Park, K.; Dai, L. Liquid crystalline polymers for efficient bilayer-bulk-heterojunction solar cells. *J. Phys. Chem. C* **2009**, *113*, 7892−7897.

(7) Conger, B. M.; Mastrangelo, J. C.; Chen, S. H. Fluorescence behavior of low molar mass and polymer liquid crystals in ordered solid films. *Macromolecules* **1997**, *30*, 4049−4055.

(8) Zhao, D. Y.; He, H. X.; Gu, X. G.; Guo, L.; Wong, K. S.; Lam, J. W. Y.; Tang, B. Z. Circularly Polarized Luminescence and a Reflective Photoluminescent Chiral Nematic Liquid Crystal Display Based on an Aggregation-Induced Emission Luminogen. *Adv. Opt. Mater.* **2016**, *4*, 534−539.

(9) Hayasaka, H.; Tamura, K.; Akagi, K. Dynamic switching of linearly polarized emission in liquid-crystallinity-embedded photo-responsive conjugated polymers. *Macromolecules* **2008**, *41*, 2341−2346.

(10) Seo, J.; Kim, S.; Gihm, S. H.; Park, C. R.; Park, S. Y. Highly fluorescent columnar liquid crystals with elliptical molecular shape: oblique molecular stacking and excited-state intramolecular proton-transfer fluorescence. *J. Mater. Chem.* **2007**, *17*, 5052−5057.

(11) Vijayaraghavan, R. K.; Abraham, S.; Akiyama, H.; Furumi, S.; Tamaoki, N.; Das, S. Photoresponsive Glass-Forming Butadiene-Based Chiral Liquid Crystals with Circularly Polarized Photoluminescence. *Adv. Funct. Mater.* **2008**, *18*, 2510−2517.

(12) Whitehead, K.; Grell, M.; Bradley, D.; Inbasekaran, M.; Woo, E. Polarized emission from liquid crystal polymers. *Synth. Met.* **2000**, *111-112*, 181−185.

(13) Belletête, M.; Bouchard, J.; Leclerc, M.; Durocher, G. Photophysics and solvent-induced aggregation of 2, 7-carbazole-based conjugated polymers. *Macromolecules* **2005**, *38*, 880−887.

(14) Borisov, S. M.; Wolfbeis, O. S. Optical biosensors. *Chem. Rev.* **2008**, *108*, 423−461.

(15) Domaille, D. W.; Que, E. L.; Chang, C. J. Synthetic fluorescent sensors for studying the cell biology of metals. *Nat. Chem. Biol.* **2008**, *4*, 168−175.

(16) Giepmans, B. N.; Adams, S. R.; Ellisman, M. H.; Tsien, R. Y. The fluorescent toolbox for assessing protein location and function. *Science* **2006**, *312*, 217−224.

(17) Jakubiak, R.; Collison, C. J.; Wan, W. C.; Rothberg, L. J.; Hsieh, B. R. Aggregation quenching of luminescence in electroluminescent conjugated polymers. *J. Phys. Chem. A* **1999**, *103*, 2394−2398.

(18) Lemmer, U.; Heun, S.; Mahrt, R.; Scherf, U.; Hopmeier, M.; Siegner, U.; Göbel, E.; Müllen, K.; Bässler, H. Aggregate fluorescence in conjugated polymers. *Chem. Phys. Lett.* **1995**, *240*, 373−378.

(19) Thomas, S. W.; Joly, G. D.; Swager, T. M. Chemical sensors based on amplifying fluorescent conjugated polymers. *Chem. Rev.* **2007**, *107*, 1339−1386.

(20) Valeur, B.; Berberan-Santos, M. N. *Molecular Fluorescence: Principles and Applications*; John Wiley & Sons: 2012.

(21) Sapsford, K. E.; Berti, L.; Medintz, I. L. Molecular fluorescence: principles and applications. *Angew. Chem., Int. Ed.* **2006**, *45*, 4562−4589.

(22) Tsujimoto, H.; Ha, D. G.; Markopoulos, G.; Chae, H. S.; Baldo, M. A.; Swager, T. M. Thermally Activated Delayed Fluorescence and Aggregation InducedEmission with Through-Space Charge Transfer. *J. Am. Chem. Soc.* **2017**, *139*, 4894−4900.

(23) Ren, Y.; Dong, Y.; Lam, J. W.; Tang, B. Z.; Wong, K. S. Studies on the aggregation-induced emission of silole film and crystal by time-resolved fluorescence technique. *Chem. Phys. Lett.* **2005**, *402*, 468−473.

(24) Luo, J. D.; Xie, Z. L.; Lam, J. W. Y.; Cheng, L.; Chen, H. Y.; Qiu, C. F.; Kwok, H. S.; Zhan, X. W.; Liu, Y. Q.; Zhu, D. B.; Tang, B. Z. Aggregation-induced emission of 1-methyl-1,2,3,4,5-pentaphenylsilole. *Chem. Commun.* **2001**, *18*, 1740−1741.

(25) Chen, Z. H.; Bouffard, J.; Kooi, S. E.; Swager, T. M. Highly Emissive Iptycene-Fluorene Conjugated Copolymers: Synthesis and Photophysical Properties. *Macromolecules* **2008**, *41*, 6672−6676.

(26) Dong, H.; Luo, M.; Wang, S.; Ma, X. Synthesis and properties of tetraphenylethylene derivatived diarylethene with photochromism and aggregation-induced emission. *Dyes Pigm.* **2017**, *139*, 118−128.

(27) Du, X.; Qi, J.; Zhang, Z.; Ma, D.; Wang, Z. Y. Efficient non-doped near infrared organic light-emitting devices based on fluorophores with aggregation-induced emission enhancement. *Chem. Mater.* **2012**, *24*, 2178−2185.

(28) Deans, R.; Kim, J.; Machacek, M. R.; Swager, T. M. A Poly(p-phenyleneethynylene) with a Highly Emissive Aggregated Phase. *J. Am. Chem. Soc.* **2000**, *122*, 8565−8566.

(29) Kim, H. Ju.; Whang, D. R.; Gierschner, J.; Lee, C. H.; Park, S. Y. High-Contrast Red−Green−Blue Tricolor Fluorescence Switching in

Bicomponent Molecular Film. *Angew. Chem., Int. Ed.* **2015**, *54*, 4330−4333.

(30) Kwok, R. T.; Leung, C. W.; Lam, J. W.; Tang, B. Z. Biosensing by luminogens with aggregation-induced emission characteristics. *Chem. Soc. Rev.* **2015**, *44*, 4228−4238.

(31) Mei, J.; Leung, N. L.; Kwok, R. T.; Lam, J. W.; Tang, B. Z. Aggregation-induced emission: together we shine, united we soar. *Chem. Rev.* **2015**, *115*, 11718−11940.

(32) Xu, S.; Liu, T.; Mu, Y.; Wang, Y. F.; Chi, Z.; Lo, C. C.; Liu, S.; Zhang, Y.; Lien, A.; Xu, J. An Organic Molecule with Asymmetric Structure Exhibiting Aggregation-Induced Emission, Delayed Fluorescence, and Mechanoluminescence. *Angew. Chem., Int. Ed.* **2015**, *54*, 874−879.

(33) Kwon, O. K.; Park, J. H.; Kim, D. W.; Park, S. K.; Park, S. Y. High Contrast Fluorescence Patterning in Cyanostilbene-Based Crystalline Thin Films: Crystallization-Induced Mass Flow Via a Photo-Triggered Phase Transition. *Adv. Mater.* **2015**, *27*, 1951−1956.

(34) An, B. K.; Kwon, S.-K.; Jung, S. D.; Park, S. Y. Enhanced Emission and Its Switching in Fluorescent Organic Nanoparticles. *J. Am. Chem. Soc.* **2002**, *124*, 14410−14415.

(35) Hong, Y.; Lam, J. W.; Tang, B. Z. Aggregation-induced emission: phenomenon, mechanism and applications. *Chem. Commun.* **2009**, *29*, 4332−4353.

(36) Hong, Y.; Lam, J. W.; Tang, B. Z. Aggregation-induced emission. *Chem. Soc. Rev.* **2011**, *40*, 5361−5388.

(37) Liu, J.; Lam, J. W.; Tang, B. Z. Acetylenic polymers: syntheses, structures, and functions. *Chem. Rev.* **2009**, *109*, 5799−5867.

(38) Wang, M.; Zhang, G.; Zhang, D.; Zhu, D.; Tang, B. Z. luorescent bio/chemosensors based on silole and tetraphenylethene luminogens with aggregation-induced emission feature. *J. Mater. Chem.* **2010**, *20*, 1858−1867.

(39) Zhao, Z.; Lam, J. W.; Tang, B. Z. Tetraphenylethene: a versatile AIE building block for the construction of efficient luminescent materials for organic light-emitting diodes. *J. Mater. Chem.* **2012**, *22*, 23726−23740.

(40) Zhao, Z.; Lam, J. W. Y.; Zhong Tang, B. Aggregation-induced emission of tetraarylethene luminogens. *Curr. Org. Chem.* **2010**, *14*, 2109−2132.

(41) Xu, Y.; Chen, L.; Guo, Z.; Nagai, A.; Jiang, D. Light-emitting conjugated polymers with microporous network architecture: interweaving scaffold promotes electronic conjugation, facilitates exciton migration, and improves luminescence. *J. Am. Chem. Soc.* **2011**, *133*, 17622−17625.

(42) Krikorian, M.; Liu, S.; Swager, T. M. Columnar Liquid Crystallinity and Mechanochromism in Cationic Platinum(II) Complexes. *J. Am. Chem. Soc.* **2014**, *136*, 2952−2955.

(43) O'Neill, M.; Kelly, S. M. Liquid crystals for charge transport, luminescence, and photonics. *Adv. Mater.* **2003**, *15*, 1135−1146.

(44) Park, J. W.; Nagano, S.; Yoon, S. J.; Dohi, T.; Seo, J. W.; Seki, T.; Park, S. Y. High Contrast Fluorescence Patterning in Cyanostilbene-Based Crystalline Thin Films: Crystallization-Induced Mass Flow Via a Photo-Triggered Phase Transition. *Adv. Mater.* **2014**, *26*, 1354−1359.

(45) Tanabe, K.; Suzui, Y.; Hasegawa, M.; Kato, T. Full-Color Tunable Photoluminescent Ionic Liquid Crystals Based on Tripodal Pyridinium, Pyrimidinium, and Quinolinium Salts. *J. Am. Chem. Soc.* **2012**, *134*, 5652−5661.

(46) Sagara, Y.; Kato, T. Stimuli-Responsive Luminescent Liquid Crystals: Change of Photoluminescent Colors Triggered by a Shear-Induced Phase Transition. *Angew. Chem.* **2008**, *120*, 5253−5256.

(47) Sagara, Y.; Kato, T. Brightly Tricolored Mechanochromic Luminescence from a Single Luminophore Liquid Crystal: Reversible Writing and Erasing of Images. *Angew. Chem.* **2011**, *123*, 9294−9298.

(48) Yuan, W. Z.; Yu, Z. Q.; Lu, P.; Deng, C.; Lam, J. W.; Wang, Z.; Chen, E. Q.; Ma, Y.; Tang, B. Z. High efficiency luminescent liquid crystal: aggregation-induced emission strategy and biaxially oriented mesomorphic structure. *J. Mater. Chem.* **2012**, *22*, 3323−3326.

(49) Yuan, W. Z.; Yu, Z. Q.; Tang, Y.; Lam, J. W.; Xie, N.; Lu, P.; Chen, E. Q.; Tang, B. Z. High solid-state efficiency fluorescent main chain liquid crystalline polytriazoles with aggregation-induced emission characteristics. *Macromolecules* **2011**, *44*, 9618−9628.

(50) Kim, J. H.; Cho, S.; Cho, B. K. An Unusual Stacking Transformation in Liquid-Crystalline Columnar Assemblies of Clicked Molecular Propellers with Tunable Light Emissions. *Chem. - Eur. J.* **2014**, *20*, 12734−12739.

(51) Zhao, D.; Fan, F.; Cheng, J.; Zhang, Y.; Wong, K. S.; Chigrinov, V. G.; Kwok, H. S.; Guo, L.; Tang, B. Z. Light-Emitting Liquid Crystal Displays Based on an Aggregation-Induced Emission Luminogen. *Adv. Opt. Mater.* **2015**, *3*, 199−202.

(52) Wang, S. J.; Zhao, R. Y.; Yang, S.; Yu, Z. Q.; Chen, E. Q. A complex of poly(4-vinylpyridine) and tolane based hemi-phasmid benzoic acid: towards luminescent supramolecular side-chain liquid crystalline polymers. *Chem. Commun.* **2014**, *50*, 8378−8381.

(53) Jing, H.; Lu, L.; Feng, Y. K.; Zheng, J. F.; Deng, L. D.; Chen, E. Q.; Ren, X. K. Aggregation-Induced Emission, and Liquid Crystalline Structure of Tetraphenylethylene−Surfactant Complex via Ionic Self-Assembly. *J. Phys. Chem. C* **2016**, *120*, 27577−27586.

(54) Hu, R.; Leung, N. L.; Tang, B. Z. AIE macromolecules: syntheses, structures and functionalities. *Chem. Soc. Rev.* **2014**, *43*, 4494−4562.

(55) Beneduci, A.; Cospito, S.; La Deda, M.; Veltri, L.; Chidichimo, G. Electrofluorochromism in π-conjugated ionic liquid crystals. *Nat. Commun.* **2014**, DOI: 10.1038/ncomms4105.

(56) Fujisawa, K.; Okuda, Y.; Izumi, Y.; Nagamatsu, A.; Rokusha, Y.; Sadaike, Y.; Tsutsumi, O. Reversible thermal-mode control of luminescence from liquid-crystalline gold (I) complexes. *J. Mater. Chem. C* **2014**, *2*, 3549−3555.

(57) Wang, Y. F.; Shi, J.; Chen, J.; Zhu, W. G.; Baranoff, E. Recent progress in luminescent liquid crystal materials: design, properties and application for linearly polarised emission. *J. Mater. Chem. C* **2015**, *3*, 7993−8005.

(58) Zhou, Q. F.; Li, H. M.; Feng, X. D. Synthesis of liquid-crystalline polyacrylates with laterally substituted mesogens. *Macromolecules* **1987**, *20*, 233−234.

(59) Liu, Y.; Zhang, D.; Wan, X. H.; Zhou, Q. F. Synthesis of a Novel "Mesogen-Jacketed Liquid Crystal Polymer" Based on Vinylterephthatic Acid. *Chin. J. Polym. Sci.* **1998**, *16*, 283−283.

(60) Chen, X. F.; Shen, Z. H.; Wan, X. H.; Fan, X. H.; Chen, E. Q.; Ma, Y. G.; Zhou, Q. F. Mesogen-jacketed liquid crystalline polymers. *Chem. Soc. Rev.* **2010**, *39*, 3072−3101.

(61) Xie, H. L.; Jie, C. K.; Yu, Z. Q.; Liu, X. B.; Zhang, H. L.; Shen, Z. H.; Chen, E. Q.; Zhou, Q. F. Design, synthesis, and characterization of a combined main-chain/side-chain liquid crystalline polymer based on mesogen-jacketed liquid crystal polymer via atom transfer radical polymerization. *J. Am. Chem. Soc.* **2010**, *132*, 8071−8080.

(62) Ye, C.; Zhang, H. L.; Huang, Y.; Chen, E. Q.; Lu, Y.; Shen, D.; Wan, X. H.; Shen, Z.; Cheng, S. Z.; Zhou, Q. F. Molecular weight dependence of phase structures and transitions of mesogen-jacketed liquid crystalline polymers based on 2-vinylterephthalic acids. *Macromolecules* **2004**, *37*, 7188−7196.

(63) Zhu, Y. F.; Guan, X. L.; Shen, Z.; Fan, X. H.; Zhou, Q. F. Competition and promotion between two different liquid-crystalline building blocks: mesogen-jacketed liquid-crystalline polymers and triphenylene discotic liquid crystals. *Macromolecules* **2012**, *45*, 3346−3355.

(64) Weng, L.; Yan, J. J.; Xie, H. L.; Zhong, G. Q.; Zhu, S. Q.; Zhang, H. L.; Chen, E. Q. Design, synthesis, and self-assembly manipulating of polymerized ionic liquids contained imidazolium based on "Jacketing" effect. *J. Polym. Sci., Part A: Polym. Chem.* **2013**, *51*, 1912−1923.

(65) Yan, J. J.; Xie, H. L.; Weng, L.; Yang, S.; Zhang, H. L. Manipulating ordered structure of ionic liquid crystalline polymers through tuning the alkyl spacer length. *Polymer* **2014**, *55*, 6504−6512.

(66) Fan, X.; Sun, J. L.; Wang, Z. Z.; Wang, P.; Dong, Y. Q.; Hu, R. R.; Tang, B. Z.; Zou, D. C. Photoluminescence and electroluminescence of hexaphenylsilole are enhanced by pressurization in the solid state. *Chem. Commun.* **2008**, *26*, 2989−2991.